4f charge-density deformation and magnetostrictive bond strain observed in amorphous TbFe2 by x-ray absorption spectroscopy

Sakura Pascarelli, M. P. Ruffoni, Angela Trapananti, Olivier Mathon, Carsten Detlefs, M. Pasquale, A. Magni, C. P. Sasso, F. Celegato, E. Olivetti, et al.

PHYSICAL REVIEW B **81**, 020406(R) (2010)

4*f* charge-density deformation and magnetostrictive bond strain observed in amorphous $TbFe_2$ by x-ray absorption spectroscopy

S. Pascarelli,[1] M. P. Ruffoni,[1] A. Trapananti,[1] O. Mathon,[1] C. Detlefs,[1] M. Pasquale,[2] A. Magni,[2] C. P. Sasso,[2] F. Celegato,[2] E. Olivetti,[2] Y. Joly,[3] and D. Givord[3]

[1]*European Synchrotron Radiation Facility, BP 220, F-38043 Grenoble, France*

[2]*INRIM, IENGF, Strada delle Cacce, 91 10135 Torino, Italy*

[3]*Institut NEEL, CNRS and Université Joseph Fourier, BP 166, 38042 Grenoble Cedex 9, France*

(Received 4 December 2009; published 12 January 2010)

The giant magnetostriction observed in rare-earth transition-metal compounds such as Terfenol-D ($Tb_{0.3}Dy_{0.7}Fe_2$) is commonly associated with the huge anisotropy of the 4*f* electron cloud. We report here the experimental observation of this phenomenon at the atomic scale, in amorphous matter. By using extended x-ray absorption fine structure spectroscopy in a differential mode, the bond strains resulting from the coupling between the anisotropic shape of the Tb 4*f* charge density and the environment crystalline electric field are measured. In a-$TbFe_2$ we measure Fe-Fe and Fe-Tb bond contractions equal to $6(1)\times10^{-4}$ Å and of $9(2)\times10^{-4}$ Å, respectively. These are the smallest atomic displacements ever detected in amorphous matter.

DOI: 10.1103/PhysRevB.81.020406 PACS number(s): 75.80.+q, 61.05.cj, 75.50.Kj, 75.50.Cc

In order to efficiently convert electromagnetic energy into mechanical work and vice versa, magnetostrictive transducers require strong magnetoelastic coupling.[1] This can be found, for example, in the elementary rare-earth (RE) metals (which exhibit strains up to $\Delta l/l \sim 7500\times10^{-6}$) as well as in RE alloys.[2,3] The strain is thought to arise from the highly anisotropic 4*f* charge distribution, which couples to both the 4*f* magnetic moment (through the spin-orbit interaction) and the surrounding atoms (via the so-called crystalline electric field, CEF). Changes in size or orientation of the RE magnetic moment are reflected in a change of the 4*f* charge distribution, which in turn forces the surrounding atoms to attain new equilibrium positions, minimizing the total energy. The end result is a large magnetostrictive strain.[4]

Although the fundamental mechanism driving magnetostriction has been known for many years, experimental evidence of the coupling between changes in the 4*f* charge density and the resulting changes in near neighbor bond lengths is still lacking. This is primarily due to the difficulty in finding a suitable probe with which to measure strains at an atomic scale. In this Rapid Communication, we give the experimental proof of this mechanism by simultaneously measuring the 4*f* charge anisotropy and the changes in distances of the surrounding atoms in an amorphous material. We used $TbFe_2$, a RE-Fe compound which is magnetic at room temperature and presents significant advantages over the RE metals. Due to the RE metals' low Curie temperature (T_c) and high magnetocrystalline anisotropy (MCA), strong magnetostriction is only seen at low temperatures and in large fields. Much work in recent decades has focused on the study of cubic Laves (or C15) phase $RE\text{-}Fe_2$ compounds, with Curie temperature $T_c \approx 700$ K, in an attempt to manufacture high-strain devices that operate at room temperature (RT). Low MCA, inherent to cubic symmetry, permits magnetostriction to be revealed in modest fields. For a review see Ref. 5.

In the $RE\text{-}Fe_2$ structure, the local symmetry at the rare-earth site is such that a rhombohedral [111] distortion is more strongly favored than a tetragonal [100] distortion: $|\lambda_{111}/\lambda_{100}| \gg 1$ where λ_{111} and λ_{100} are the relative deformations along [111] and [100], respectively. Thus, in polycrystalline materials, the magnetostriction and magnetomechanical coupling is strongly dependent upon crystallite orientation. Within this family, the crystalline compound $TbFe_2$ (c-$TbFe_2$) has the largest intrinsic zero kelvin magnetostriction, exceeding $\Delta l/l \sim 4000\times10^{-6}$.[6] Because of strong Fe-Fe and Fe-Tb exchange interactions, more than half of this magnetostriction is preserved at RT (T_c=698 K).

The mechanism for these magnetoelastic distortions was explained 40 years ago by Cullen and Clark,[7] who demonstrated that in $TbFe_2$, an internal displacement involving the shift of Tb atoms along the [111] direction is the only infinite wavelength internal mode that can couple to the RE orbital moment. This displacement lowers the symmetry and drives the external rhombohedral distortion.[8] According to this picture, internal shifts of the Fe atoms are negligible since they couple to neither the orbital momenta nor the external strains. Recent *ab initio* calculations[9] have provided reasonable agreement with the observed magnetostriction, but again experimental proof of the underlying mechanism is missing.

In this study, amorphous, rather than polycrystalline, $TbFe_2$ was chosen. The mechanisms which govern magnetostriction in the cubic $RE\text{-}Fe_2$ compounds are essentially preserved in the amorphous state, while the problem of crystallite orientation strongly affecting the magnetostriction in crystalline systems is avoided. Samples were deposited on a 200 μm vitreous carbon substrate by RF sputtering in an Ar plasma until the optimal thickness of ~6 micrometers required for the measurements was obtained. The films were peeled off their substrate, and quantitative microanalysis used to determine their elemental composition (72 at. % Fe, and 28 at. % Tb). X-ray diffraction confirmed their amorphous nature.

Since the structural disorder inherent to the amorphous phase suppresses any macroscopic anisotropy, there is considerable interest in the application of such amorphous materials [Ref. 10 and references therein]. In amorphous $TbFe_2$

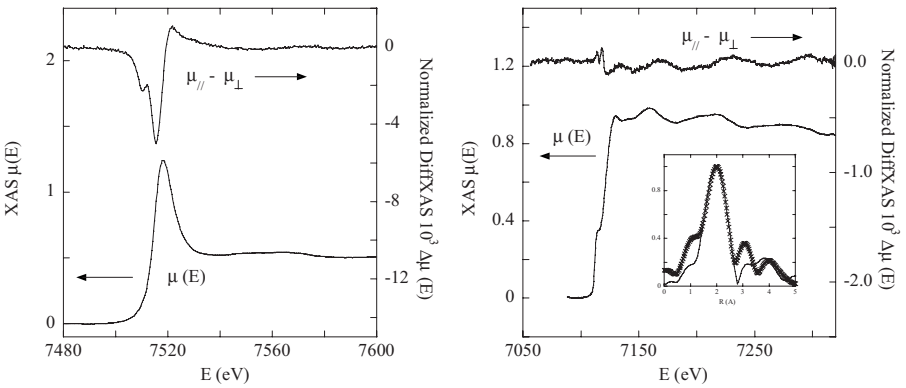

FIG. 1. (a) Raw Tb L_3 edge XAS signal $\mu(E)$ and normalized DiffXAS $\Delta\mu(E)=\mu^{\|}$-$\mu^{\perp}$. (b) Raw Fe K edge XAS signal $\mu(E)$ and normalized DiffXAS $\Delta\mu(E)=\mu^{\|}$-$\mu^{\perp}$. The inset compares the Fourier transform of the EXAFS (line) and DiffXAS (crosses) oscillations.

(a-$TbFe_2$), strain values of the order of $\sim 300\times 10^{-6}$ have been reported at 0.5 T.[5] Although these values are much lower than those observed in c-$TbFe_2$, they are still relatively large, in agreement with the fact that the mechanism responsible for the magnetostriction in the crystalline systems is still active in the disordered amorphous structure.

In 1996, Bonin and Crozier attempted to use x-ray absorption spectroscopy (XAS) as a microscopic strain gauge to determine which atoms contribute to the observed giant magnetostriction of Terfenol-D ($Tb_{0.3}Dy_{0.7}Fe_2$).[11] Unfortunately, no internal distortions of the unit cell were observed to within ± 0.003 Å, leading them to conclude that the resolution of the technique was insufficient for this task. However, the recent development of differential-mode XAS (DiffXAS) has changed this situation. In 2005, Pettifer *et al.* demonstrated that the sensitivity of XAS could be enhanced by about two orders of magnitude by using a dispersive XAS spectrometer coupled to a high brilliance synchrotron source.[12] DiffXAS was then further developed to investigate magnetoelastic coupling in 3*d* metals[13] and then to address the enigmatic question of the origin of enhanced magnetostriction in the technologically attractive Galfenol ($Ga_{0.2}Fe_{0.8}$) system[14] where magnetostrictive constants λ in the environment of a specific atom could be quantified. λ, however, describes a "lattice" property, not an "atomic" property, reflecting the average behavior over a number of different bonds which can individually show positive or negative strain. In the present work, the first on amorphous matter, the isotropic nature of the sample allowed us to apply a data analysis procedure based on the standard extended x-ray absorption fine structure (EXAFS) analysis to extract directly the first shell bond strains. This precise knowledge of the amplitude and sign of the changes in individual bond lengths allows, on the one hand, theoretical predictions of atomic behavior to be experimentally verified, and on the other, an understanding to be developed regarding which atomic movements are responsible for the macroscopic effects that we observe.

The XAS and DiffXAS measurements were performed at beamline ID24 of the European Synchrotron Radiation Facility.[15] For the DiffXAS measurements, the sample was placed at the center of a 0.5 T magnetic field, which rotated in the plane perpendicular to the propagation of linearly polarized x rays. The absorption coefficient, $\mu(E)$, was recorded with the magnetic field direction **B** parallel and then perpendicular, $\mu^{\|}(E)$ and $\mu^{\perp}(E)$, respectively, to the x-ray electric-field polarization vector **E**. The differential absorption, $\Delta\mu(E)=\mu^{\|}(E)$-$\mu^{\perp}(E)$, averaged over a large number of cycles to improve the signal-to-noise ratio, was normalized by dividing by the edge jump. The changes in bond lengths derived from $\Delta\mu(E)$ are thus the average differences in length, projected along **E**, resulting from a 90° rotation of the applied magnetic field.

Figures 1(a) and 1(b) show the raw Tb L_3 and Fe K edge absorption spectra $\mu(E)$ and the normalized DiffXAS $\Delta\mu(E)$. At the Tb L_3 edge, the differential signal $\Delta\mu(E)$ is dominated by a large x-ray magnetic linear dichroism (XMLD) signal[16] at the absorption onset, of peak-peak amplitude $|\Delta\mu|_{\text{P-P}}\sim 5\times 10^{-3}$. $\Delta\mu(E)$ features a major peak at 7515 eV, with a well resolved shoulder at 7510 eV. In the absorption spectrum $\mu(E)$ however, a single resonance is observed, corresponding to the onset of the dipole allowed $2p\rightarrow 5d$ transition.

At the Fe K edge, the XMLD signal at the absorption onset is much weaker, $|\Delta\mu|_{\text{P-P}}\sim 2\times 10^{-4}$, and $\Delta\mu(E)$ is dominated by the differential EXAFS oscillations that extend for over 200 eV beyond the edge. To analyze this signal, we first performed a standard EXAFS data analysis[17] to extract the "average" local structure in the environment of Tb and Fe, by fitting simultaneously the EXAFS signals $\chi(k)$ extracted from the absorption spectra $\mu(E)$ at both edges. By Fourier filtering the $\chi(k)$ oscillations, we found that the signal in R-space extends only up to about 3.0 Å from the Fe or Tb absorber, with information from larger distances being washed out due to the large structural disorder intrinsic to amorphous matter. The EXAFS is therefore not sensitive to Tb-Tb interactions at $R_{\text{TbTb}}\sim 3.2$ Å. For both edges, $\chi(k)$ could be reproduced well in this frequency range using a model based on the structure of c-$TbFe_2$, where Fe is surrounded by six Fe and six Tb atoms at distances $R_{\text{FeFe}}=2.60$ Å and $R_{\text{FeTb}}=3.05$ Å. Coordination numbers were fixed to their nominal values in the crystal. Fitted parameters were bond distances R_{FeFe} and R_{FeTb}, mean-square relative displacements $\Delta\sigma^2_{\text{FeFe}}$ and $\Delta\sigma^2_{\text{FeTb}}$, and a common energy offset ΔE. Best fit parameters were $R_{\text{FeFe}}=2.48(1)$ Å, $\Delta\sigma^2_{\text{FeFe}}=17(1)\times 10^{-3}$ Å^2, $R_{\text{FeTb}}=3.05(3)$ Å, $\Delta\sigma^2_{\text{FeTb}}=35(5)\times 10^{-3}$ Å^2, $\Delta E=4(1)$ eV. The results are shown in Fig. 2(a). The local environment around Fe and Tb can therefore be described quite well by a disordered "Laves phase" structure, with a slight contraction (−5%) of the Fe-Fe bonds and with large static disorder, especially on the Tb positions. Our results are consistent with the early EXAFS work of Stern *et al.*[18] on a-RE-Fe_2 compounds.

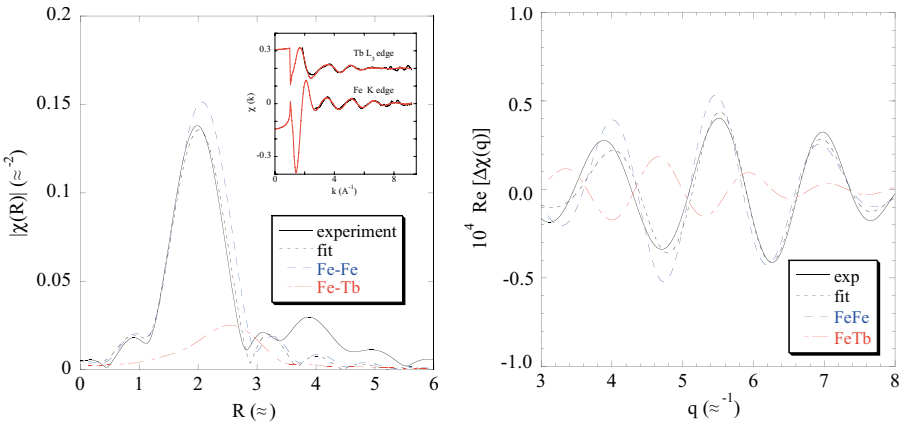

FIG. 2. (Color online) (a) Amplitude of Fourier transform $|\chi(R)|$ of the Fe K-edge EXAFS compared to best fit Fe-Fe (dash blue), Fe-Tb (dash-dot red), and sum (dot black) components. Note that the R axis is not phase shift corrected ($\Delta R \sim +0.5$ Å). The inset shows the $\chi(k)$ signals compared to the best fit at both edges. (b) Best fit to the filtered DiffXAS signal. Filtered signal Re$[\Delta\chi(q)]$ and best fit (black line and dot line). Fe-Fe (dash blue) and Fe-Tb component (dash-dot red).

Given the average local structural parameters, we then analyzed the DiffXAS signal $\Delta\mu(E)$ (Ref. 19) to extract values of bond strains, $\delta R = R^{\parallel} - R^{\perp}$, for both Fe-Fe and Fe-Tb. The best fit, shown in Fig. 2(b), yields strain values $\delta R_{\mathrm{FeFe}}/R_{\mathrm{FeFe}} = -230(40) \times 10^{-6}$ and $\delta R_{\mathrm{FeTb}}/R_{\mathrm{FeTb}} = -340(80) \times 10^{-6}$. The sign of the atomic Fe-Fe and Fe-Tb magnetostrictive strain is negative, in agreement with the earlier (though inconclusive) EXAFS experiment on Terfenol-D,[11] but opposite to that of macroscopic measurements.[5] Since the microscopic strain must build up to the observed positive macroscopic strain, we conclude that the Tb-Tb strain, δR_{TbTb}, must be much larger than δR_{FeFe} and δR_{FeTb}, and that it must be positive.

Since our EXAFS data was not sensitive to the Tb-Tb bond, we tried to extract some information on the Tb-Tb strain from the large differential signal observed around the Tb L_3 white line. We performed *ab initio* calculations using a monoelectronic, Muffin Tin potential in the framework of fully relativistic multiple-scattering theory,[20] thus including the spin-orbit interaction. The calculation was based on a small cluster of c-$TbFe_2$ of radius equal to 3.1 Å, encompassing the central Tb and its 12 Fe neighbors at $R_{\mathrm{Tb\text{-}Fe}} = 3.05$ Å. This was then extended to 4.0 Å to include the 4 Tb neighbors at $R_{\mathrm{TbTb}} = 3.2$ Å. The calculation is *ab initio* in the sense that from the atomic cluster and the orientation of the atomic magnetic moments (assumed to be aligned with the external magnetic field), no other parameters are used to solve the Dirac (or Schrödinger-like) equation. The resulting electronic structure permits the calculation of the transition matrices and the absorption cross section. Static disorder was not included, but the signal was averaged over a set of randomly oriented crystallites, to take into account the isotropic nature of our sample.

We carried out calculations for the nominal c-$TbFe_2$ structure (with all atoms at their equilibrium positions) as well as for an "internally distorted" structure, involving a displacement of the Tb atom from its equilibrium position along the [111] direction when $\mathbf{B} \parallel [111]$, and no displacement when $\mathbf{B} \perp [111]$. In the left panel of Fig. 3 we compare the experimental $\Delta\mu(E)$ (bottom) with the result of the calculation for the undistorted structure for the 3.1 (top) and 4.0 Å (middle) cluster. The amplitude and shape of the signal are correctly reproduced only when the calculation includes the four Tb-Tb bonds, indicating that it is particularly sensitive to the Tb-Tb interaction. The main peak at 7515 eV corresponding to the $2p \rightarrow 5d$ dipole transition arises from an electric-quadrupole moment carried by the Tb $5d$ electrons, i.e., a difference in the $5d$ electron-density projected $\parallel\mathbf{B}$ and $\perp\mathbf{B}$. The shoulder at 7510 eV, found to be associated with the dipole-forbidden $2p \rightarrow 4f$ transition, is invisible in the absorption spectrum but strongly highlighted in the XMLD. This implies that a major change occurs also in the projection of the $4f$ electron density. Such a result is expected for M-rich RE-M alloys (M=Fe or Co), where, due to the predominance of the RE-M exchange interactions over CEF interactions, the $4f$ electron density is not rigidly clamped to the lattice but rotates together with the $4f$ moments. The agreement in shape and intensity between the calculation and the experiment is excellent (no scale adjustment parameter was used on either axis) considering the crudeness of the potential used, and the approximations made to simulate the amorphous structure (no structural disorder).

In the right panel of Fig. 3, we introduce displacements of the Tb from its equilibrium position, and see that the amplitude and shape of the peak at 7515 eV is particularly sensitive to its position. The red and green lines correspond to $\delta R_{\mathrm{TbTb}}/R_{\mathrm{TbTb}} = +8200 \times 10^{-6}$ (red) and -8200×10^{-6} (green)

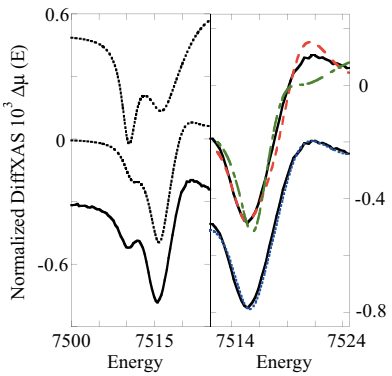

FIG. 3. (Color online) Left panel. Experimental Tb L_3 $\Delta\mu(E)$ (solid line bottom) and simulations for an undistorted structure using a 4.0 Å (dashed line middle) and 3.1 Å (dashed line top) cluster. Right panel: $\Delta\mu(E)$ (black) compared to simulations using different displacements of Tb along the [111] direction: $\delta R_{\mathrm{Tb\text{-}Tb}}/R_{\mathrm{Tb\text{-}Tb}} = +8200 \times 10^{-6}$ (dash red), -8200×10^{-6} (dash-dot green). Best agreement is found for $\delta R_{\mathrm{Tb\text{-}Tb}}/R_{\mathrm{Tb\text{-}Tb}} = +2500 \times 10^{-6}$ (dot blue)

respectively. The best agreement with experiment was obtained for $\delta R_{\mathrm{TbTb}}/R_{\mathrm{TbTb}} \sim +2500 \times 10^{-6}$ (blue), indicating an important elongation of the Tb-Tb bond. This finding, although qualitative, is important because it adds consistency to our quantitative Fe *K*-edge data analysis.

The large positive Tb-Tb strain is in agreement with the early work of Cullen and Clark.[7] However, the authors did not foresee any displacement of Fe atoms in the crystal. Our measurements unequivocally detect a displacement of Fe atoms in our amorphous samples. According to Coehoorn,[21] the MCA in RE alloys may be understood by considering the coupling between the 4*f* orbitals and the on-site aspherical valence electron charge density. In RE-*M* alloys, the valence electron charge density at a given RE site is higher along a direction toward *M* atoms, characterized by a high valence electron number, and lower toward RE atoms, characterized by a lower valence electron number. Since magnetostriction is the process by which a strain develops to further minimize the MCA energy, for RE elements (such as Tb) having an oblate 4*f* shell, RE-RE (RE-*M*) bonds are positively (negatively) strained when the moment is directed toward the bond direction and negatively strained in the other case. Thus, δR_{TbFe} must be negative and δR_{TbTb} positive, in agreement with experiment. In this discussion, the Fe-Fe bond strain is not directly involved. To explain the observed negative δR_{FeFe}, it should be considered that the magnetostrictive deformation works against elastic energy. To minimize the elastic energy, the Fe-Fe strain is expected to be of opposite sign to the dominant positive Tb-Tb strain. In conclusion, by strain measurement at an atomic level in amorphous matter, we have experimentally revealed the coupling between a change in the shape of the anisotropic 4*f* charge density and the resulting change in near neighbor bond lengths. In a-$TbFe_2$ the derived elongation of the Tb-Tb bond is of the order of 8×10^{-3} Å and the Fe-Fe and Fe-Tb bond contractions are equal to $6(1) \times 10^{-4}$ Å and $9(2) \times 10^{-4}$ Å, respectively. These are the smallest atomic displacements ever detected in amorphous matter. The measurement of such displacement in amorphous magnetic materials provides a unique tool to analyze the coupling that exists between magnetic and elastic properties at the atomic scale. In principle, in ordered systems, XRD should be able to approach the same sensitivity to strain as obtained here,[22] but no other technique to date can compete with EXAFS concerning the sensitivity to changes in nearest-neighbor bond lengths in totally disordered systems.

Potential applications of this technique within the field of magnetically anisotropic systems include investigation of Laves phases with different RE atoms, such as the giant magnetostrictive Terfenol-D ($Tb_{0.3}Dy_{0.7}Fe_2$), where the role played by the asymmetry of each RE could be analyzed separately. In systems where the contribution to anisotropy and magnetostriction from 3*d* magnetism is large, the measurement of *M*-*M* local displacement could help in determining the symmetry of the dominant 3*d* orbitals. Beyond magnetic anisotropy, the ability to measure tiny atomic displacements opens many opportunities to examine magnetoelastic coupling in general. Among potential systems are Invar alloys such as Fe-Ni, Fe_3Pt or RE_2Fe_{17} or systems where a transition between two magnetic states exists. As shown for the case of an amorphous system, an important aspect of the present analysis lies is the fact that the fundamental anisotropic character of the considered interactions is not hidden by the isotropic character of the average system. This is very significant considering that a strong interest presently exists for magnetic materials characterized by a certain degree of intrinsic disorder (frustrated magnetic systems, small aggregates, interfacial exchange bias, etc.).

We are grateful to Francois de Bergevin, Art Clark, and Kristl Hathaway for fruitful discussions. We thank Michela Brunelli (ESRF, then Institut Laue Langevin, Grenoble, France) for XRD characterization on beamline ID31. Finally, we are very grateful to Sebastien Pasternak and to Florian Perrin for their excellent technical assistance.

[1] L. D. Landau and E. M. Lifshitz, *Electrodynamics of Continuous Media: Course of Theoretical Physics*, 2nd Ed. (Elsevier Butterworth-Heineman, Burlington, MA, 1984), Vol. 8.
[2] S. Legvold, J. Alstad, and J. Rhyne, Phys. Rev. Lett. **10**, 509 (1963).
[3] A. E. Clark, R. Bozorth, and B. De Savage, Phys. Lett. **5**, 100 (1963).
[4] S. Buck and M. Fahnle, Phys. Rev. B **57**, R14044 (1998).
[5] A. E. Clark, in *Magnetostrictive Rare Earth*-Fe_2 *Compounds*, edited by E. P. Wohlfarth (North Holland Publishing Company, New York, 1980), Vol. 1, Chap. 7.
[6] A. E. Clark and H. S. Belson, Phys. Rev. B **5**, 3642 (1972).
[7] J. R. Cullen and A. E. Clark, Phys. Rev. B **15**, 4510 (1977).
[8] A. E. Dwight and C. W. Kimball, Acta Crystallogr., Sect. B: Struct. Crystallogr. Cryst. Chem. **30**, 2791 (1974).
[9] S. Buck and M. Fahnle, J. Magn. Magn. Mater. **204**, 1 (1999).
[10] M. Pasquale *et al.*, J. Magn. Magn. Mater. **215-216**, 769 (2000).
[11] Y. R. Bonin and E. D. Crozier, Can. J. Phys. **74**, 295 (1996).
[12] R. F. Pettifer *et al.*, Nature (London) **435**, 78 (2005).
[13] S. Pascarelli, M. P. Ruffoni, A. Trapananti, O. Mathon, G. Aquilanti, S. Ostanin, J. B. Staunton, and R. F. Pettifer, Phys. Rev. Lett. **99**, 237204 (2007).
[14] M. P. Ruffoni, S. Pascarelli, R. Grössinger, R. Sato Turtelli, C. Bormio-Nunes, and R. F. Pettifer, Phys. Rev. Lett. **101**, 147202 (2008).
[15] S. Pascarelli *et al.*, J. Synchrotron Radiat. **13**, 351 (2006).
[16] B. T. Thole, G. van der Laan, and G. A. Sawatzky, Phys. Rev. Lett. **55**, 2086 (1985); G. van der Laan, B. T. Thole, G. A. Sawatzky, J. B. Goedkoop, J. C. Fuggle, J. M. Esteva, R. Karnatak, J. P. Remeika, and H. A. Dabkowska, Phys. Rev. B **34**, 6529 (1986).
[17] A. L. Ankudinov, B. Ravel, J. J. Rehr, and S. D. Conradson, Phys. Rev. B **58**, 7565 (1998).
[18] E. Stern *et al.*, J. Magn. Magn. Mater. **7**, 188 (1978).
[19] M. P. Ruffoni, J. Synchrotron Radiat. **16**, 591 (2009).
[20] Y. Joly, Phys. Rev. B **63**, 125120 (2001).
[21] R. Coehoorn, J. Magn. Magn. Mater. **99**, 55 (1991).
[22] S. Yang and Xiaobing Ren, Phys. Rev. B **77**, 014407 (2008).